Chinese Journal of Cancer

Original Article

Nasopharyngeal adenoid cystic carcinoma: magnetic resonance imaging features in ten cases

Xue-Wen Liu[1,2*], Chuan-Miao Xie[1,2*], Hui Li[1,2], Rong Zhang[1,2], Zhi-Jun Geng[1,2], Yun-Xian Mo[1,2], Jing Zhao[1,2], Mu-Yan Cai[1,3], Yan-Chun Lv[1,2] and Pei-Hong Wu[1,2]

Abstract

Nasopharyngeal adenoid cystic carcinoma (NACC) is a rare malignancy with high local invasiveness. To date, there is no consensus on the imaging characteristics of NACC. To address this, we retrospectively reviewed 10 cases of NACC and summarized the magnetic resonance imaging (MRI) features. MR images of 10 patients with histologically validated NACC were reviewed by two experienced radiologists. The location, shape, margin, signal intensity, lesion texture, contrast enhancement patterns, local invasion, and cervical lymphadenopathy of all tumors were evaluated. Clinical and pathologic records were also reviewed. No patients were positive for antibodies against Epstein-Barr virus (EBV). The imaging patterns of primary tumors were classified into two types as determined by location, shape, and margin. Of all patients, 7 had tumors with a type 1 imaging pattern and 3 had tumors with a type 2 imaging pattern. The 4 tubular NACCs were all homogeneous tumors, whereas 3 (60%) of 5 cribriform NACCs and the sole solid NACC were heterogeneous tumors with separations or central necrosis on MR images. Five patients had perineural infiltration and intracranial involvement, and only 2 had cervical lymphadenopathy. Based on these results, we conclude that NACC is a local, aggressive neoplasm that is often negative for EBV infection and associated with a low incidence of cervical lymphadenopathy. Furthermore, MRI features of NACC vary in locations and histological subtypes.

Key words Neoplasm of the nasopharynx, adenoid cystic carcinoma, magnetic resonance imaging (MRI)

Adenoid cystic carcinoma (ACC) was first described by Billroth in 1856 and deemed cylindroma. Since then, this type of cancer has been called many other names, but the term ACC has gained general acceptance in recent years. ACC is the most common malignancy of the submandibular and minor salivary glands, but it also occurs in other glandular tissues, such as lacrimal glands, Bartholin's glands, ceruminous glands of the external auditory canal, and glands of the esophagus, breast, prostate, and cervix. ACC accounts for less than 1% of all head and neck cancers and less than 10% of all salivary gland neoplasms, but it accounts for about 40% of all malignancies of the salivary glands[1]. Nasopharyngeal adenoid cystic carcinoma (NACC) is a rare malignancy of the nasopharynx, with primary nasopharyngeal adenocarcinoma (including NACC) representing less than 0.48% of all nasopharyngeal malignancies[2].

We have noted in our daily clinical imaging practice that NACC can be easily misdiagnosed as nasopharyngeal squamous cell carcinoma (NSCC). Although a few previous studies have reported the imaging features of ACC in major salivary glands[3,4], imaging literature on NACC is limited. Most previous reports regarding NACC described either the imaging

Authors' Affiliations: [1]State Key Laboratory of Oncology in South China, Guangzhou, Guangdong 510060, P. R. China; [2]Medical Imaging and Minimally Invasive Interventional Center, [3]Department of Pathology, Sun Yat-sen University Cancer Center, Guangzhou, Guangdong 510060, P. R. China.

*These two authors contributed equally to this work.

Corresponding Author: Pei-Hong Wu, Medical Imaging and Minimally Invasive Interventional Center, Sun Yat-sen University Cancer Center, 651 Dongfeng Road East, Guangzhou, Guangdong 510060, P. R. China. Tel: +86-20-87343272; Fax: +86-20-87343272; Email: wuph@sysucc.org.cn.

doi: 10.5732/cjc.011.10242

features in a single case or the clinical experience [5,6]. Clear consensus on the imaging characteristics of NACC has not been reached. In this study, we summarized the magnetic resonance imaging (MRI) features in 10 patients with histologically validated NACC.

Patients and Methods

Patient information

Ten patients with histologically confirmed NACC were treated at the Sun Yat-sen University Cancer Center between November 2007 and February 2010. This study was approved by our Institutional Review Board. Informed consent was obtained from all patients. The clinical records of these patients, including age, sex, clinical symptoms, nasopharyngeal fiberscope reports, laboratory examinations, treatments, and follow-up information, were reviewed. The diagnosis was made based on histological examinations of biopsy specimens collected from primary nasopharyngeal tumors. Three subtypes, tubular, cribriform, and solid, were classified according to the degree of cellular differentiation. All patients were restaged according to the 2002 American Joint Committee on Cancer (AJCC) staging system for nasopharyngeal carcinoma.

Imaging protocol

All patients underwent MRI scans of the nasopharynx and neck before treatment. MRI was performed using a 1.5 Tesla unit (Signa Horizon LX Highspeed or Signa Horizon DX Highspeed, General Electric Medical Systems, USA) with a head and neck combined coil. For all patients, the following sequences were obtained: non–contrast-enhanced T1-weighted images (T1WI) in the axial, coronal, and sagittal planes; non–contrast-enhanced T2-weighted images (T2WI) in the axial plane; contrast-enhanced T1WI in the axial and sagittal planes; and contrast-enhanced fat-suppressed T1WI in the coronal plane. Gadopentate dimeglumine (0.1 mmol/kg of body weight) was administered by intravenous bolus injection for contrast-enhanced sequences.

The imaging sequences were performed with the parameters described here. Non–contrast-enhanced T1-weighted fast spin-echo (FSE) images in the axial, sagittal, and coronal planes were obtained, with repetition time/echo time of 420–450 ms/minimum full, 2 excitations, a 22 cm field of view (FOV), a 320 × 224 frequency matrix, a 5.0 mm thick section, and a 1.0 mm intersection gap. Non–contrast-enhanced axial T2-weighted FSE images in the axial plane were obtained, with repetition time/echo time of 3200–3500 ms/85 ms, 2 excitations, a 22 cm FOV, a 320 × 224 frequency matrix, a 5.0 mm thick section, and a 1.0 mm intersection gap. Contrast enhanced T1-weighted images in the axial and sagittal planes and contrast enhanced fat-suppressed T1-weighted images in the coronal plane were obtained, with repetition time/echo time of 320–350 ms/minimum full, 1 excitations, a 22 cm FOV, a 512 × 224 frequency matrix, a 5.0 mm thick section, and a 1.0 mm intersection gap.

Image assessment

Two experienced radiologists evaluated the MR images. Any disagreements were resolved by consensus. All MR images were viewed on a picture archiving and communication system workstation monitor (Centricity RA1000 Workstation V.3.0, GE Healthcare).

MRI features of primary tumors MRI features of primary tumors that were evaluated included location, shape, margin (clear or unclear), signal intensity (hypointense, isointense, or hyperintense compared to adjacent muscles), lesion texture (homogeneous or heterogeneous), and contrast enhancement patterns (homogeneous or heterogeneous; strong, moderate, or absent). Contrast enhancement patterns were considered strong if the degree of enhancement was similar to that of normal mucosa, moderate if the degree of enhancement was less than that of normal mucosa, and absent if the lesion showed no signal increase. The imaging patterns of primary tumors were classified into two types as determined by location, shape, and margins: type 1, an irregular neoplasm with unclear margin in one or several walls of the nasopharynx (Figure 1); and type 2, a regular neoplasm with clear margin (type 2a) (Figure 2) or an irregular neoplasm with unclear margin (type 2b) (Figure 3) in the parapharyngeal space.

Evaluation of local invasion on MRI Tumor invasion of regional structures included involvement of the nasal concha, paranasal sinus, oropharynx, parapharyngeal space, spatia masseterica, pterygopalatine fossa, skull base bone, cranial nerves, and intracalvarium. Oropharynx involvement was defined as tumor involvement below the inferior border of the Axis [7]. Parapharyngeal involvement was defined as posterolateral infiltration of tumor beyond the pharyngobasilar fascia[7]. Skull base invasion was defined as the presence of low-intensity tissue in the high-signal bone marrow on non-contrast-echanced T1WI images and with enhancement on contrast-enhanced T1WI images. Infiltration of the cranial nerves was diagnosed by thickness of the cranial nerves and enlargement of the foramina nervosas.

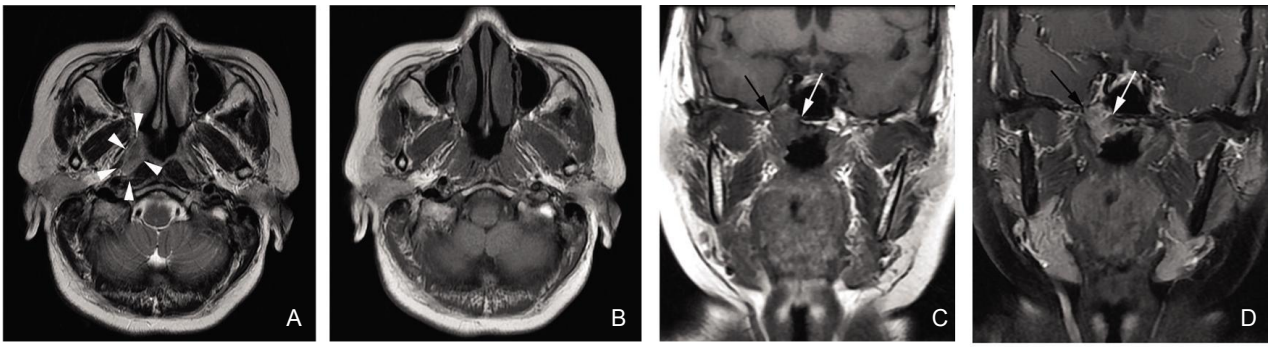

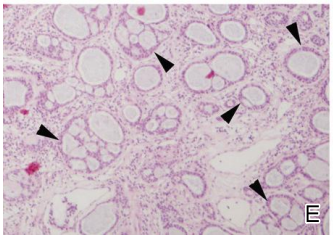

Figure 1. **Tubular subtype of nasopharyngeal adenoid cystic carcinoma (NACC) with a type 1 imaging pattern in a 56-year-old woman.** A, an axial T2-weighted fast spin-echo image (T2WI) shows an irregular lesion with unclear margin in the right wall of the nasopharynx (white arrowheads). The signal intensity of the lesion is homogenous and slightly hyperintense. B, an axial T1-weighted fast spin-echo image (T1WI) shows the signal intensity of the lesion is similar to that of muscles. C and D, a coronal T1W fast spin-echo image and a contrast-enhanced, fat-suppressed T1WI show tumor invasion in the right part of the base of the sphenoid bone (white arrows) and the right pterygoid process (black arrows), respectively. E, photomicrograph of a biopsy specimen shows the classic tubular pattern of NACC, which has many tubular structures (black arrowheads) composed of modified or neoplastic cells (HE ×40).

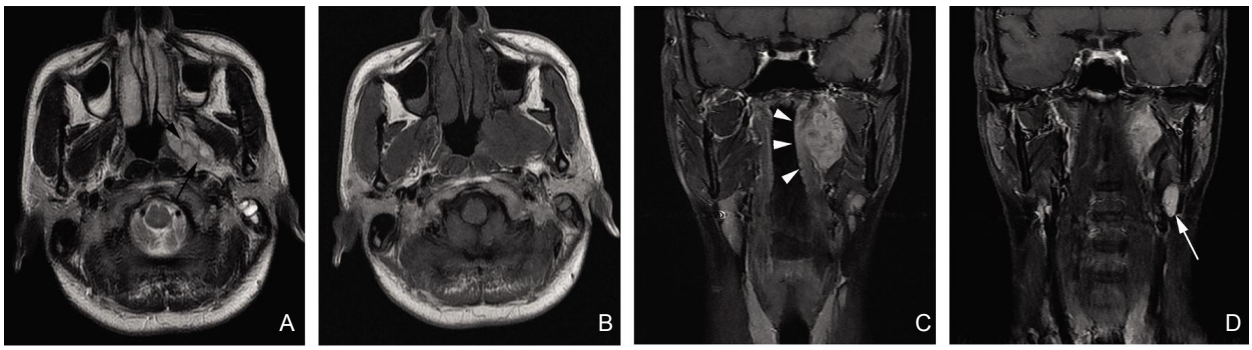

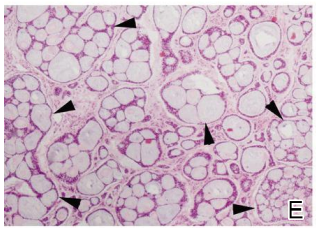

Figure 2. **Cribriform subtype of NACC with a type 2a imaging pattern in a 38-year-old man.** A, an axial T2W fast spin-echo image shows an ovoid lesion with clear margin in the left parapharyngeal space. The signal intensity of the lesion is heterogeneous and hyperintense with hypointense separations (black arrows). B, an axial T1W fast spin-echo image shows the signal intensity of the lesion is similar to that of muscles. C, a coronal contrast-enhanced, fat-suppressed T1W spin-echo image shows the lesion is localized in the left parapharyngeal space. The regional mucosa of the nasopharynx has a smooth surface (white arrowheads). D, a coronal contrast-enhanced, fat-suppressed T1W spin-echo image shows an enlarged lymph node in the left upper neck (white arrow). E, photomicrograph of a biopsy specimen shows the classic cribriform pattern of NACC, which has a Swiss cheese appearance. The gland-like spaces (black arrowheads) in the lesion clearly outnumber the tumor cells (HE ×40).

MRI criteria of cervical lymphadenopathy Regional lymphadenopathy was also evaluated. Cervical lymphadenopathy was subdivided into specific anatomic subsites according to imaging-based delineation of cervical lymph nodes[8]. The diagnosis of nodal involvement was made radiologically on the demonstration of one or more of the following criteria[9]: central necrosis, extracapsular neoplastic spread, and size (shortest axial diameter equal to or greater than 5 mm in the retropharyngeal region, 11 mm in the jugulodigastric

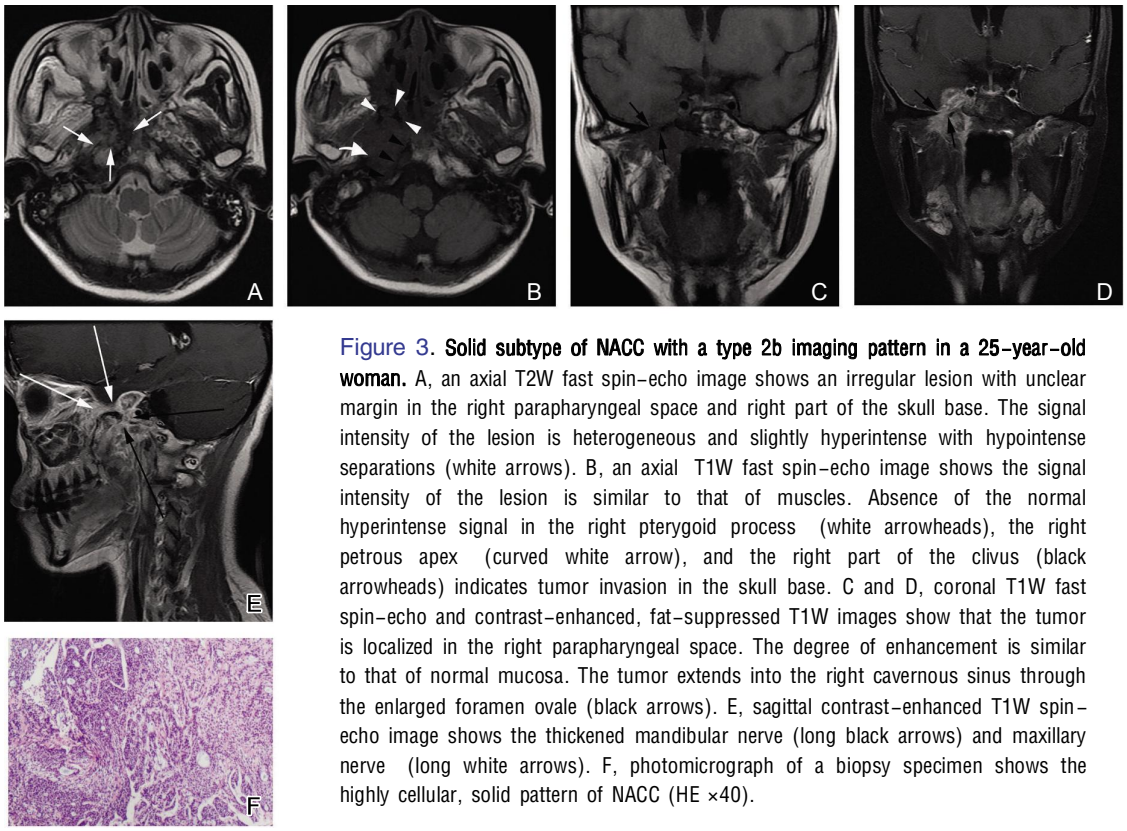

Figure 3. **Solid subtype of NACC with a type 2b imaging pattern in a 25-year-old woman.** A, an axial T2W fast spin-echo image shows an irregular lesion with unclear margin in the right parapharyngeal space and right part of the skull base. The signal intensity of the lesion is heterogeneous and slightly hyperintense with hypointense separations (white arrows). B, an axial T1W fast spin-echo image shows the signal intensity of the lesion is similar to that of muscles. Absence of the normal hyperintense signal in the right pterygoid process (white arrowheads), the right petrous apex (curved white arrow), and the right part of the clivus (black arrowheads) indicates tumor invasion in the skull base. C and D, coronal T1W fast spin-echo and contrast-enhanced, fat-suppressed T1W images show that the tumor is localized in the right parapharyngeal space. The degree of enhancement is similar to that of normal mucosa. The tumor extends into the right cavernous sinus through the enlarged foramen ovale (black arrows). E, sagittal contrast-enhanced T1W spin-echo image shows the thickened mandibular nerve (long black arrows) and maxillary nerve (long white arrows). F, photomicrograph of a biopsy specimen shows the highly cellular, solid pattern of NACC (HE ×40).

region, and 10 mm in all other regions of the neck; or a group of three or more nodes that were borderline in size in all cervical regions).

Results

Clinical characteristics

Clinical characteristics of all 10 patients are summarized in Table 1. There were 7 men and 3 women aged from 25 to 67 years (median, 51 years). The most common clinical symptoms included tinnitus (n = 6), headache (n = 4), epistaxis (n = 4), and hearing loss (n = 3). The duration of disease was variable, ranging from 0.5 to 24 months (median, 7.5 months). Trigeminal paralysis was found in 3 patients. Nasopharyngoscopic examination revealed that 8 patients had protrusions and 2 had lumps or nodular tumors in one or several walls of the nasopharynx. Of the 8 patients with protrusions in the nasopharyngeal walls, 4 had smooth protrusion surfaces and 4 had unsmooth protrusion surfaces. No patients were positive for antibodies against Epstein-Barr virus (EBV). Of the 10 cases of NACC, 4 were tubular, 5 were cribriform, and 1 was solid (Figures 1–3); I was at stage II, 3 at stage III, and 6 at stage IV. Three patients had cervical lymphadenopathy, and the only one patient with solid ACC had lung metastasis (case 10). These patients were treated with radiotherapy (n = 6), chemoradiotherapy (n = 3), or surgical resection plus radiotherapy (n = 1). Only one patient (case 3) had local recurrence in 18 months after treatment. The follow-up time ranged from 8 to 35 months and all patients were alive at the time of this investigation.

MRI features of NACCs

Imaging types of NACC MRI features of 10 patients with NACCs are listed in Table 2. Of 10 patients, 7 had tumors in one or several walls of the nasopharynx, and 3 had tumors in the parapharyngeal space. All 7 patients with tumors in the nasopharyngeal walls had irregular neoplasms with unclear margin. Of 3 patients with tumors in the parapharyngeal space, 2 had regular neoplasms with clear margin, 1 had an irregular neoplasm with unclear margin. According to these features, 7 tumors were classified into morphological type 1, and 3 were classified into type 2, which included type 2a (n = 2) and type 2b (n = 1). The 7 tumors classified as morphological type 1 included 3 tubular

Table 1. Clinical characteristics of 10 patients with Nasopharyngeal adenoid cystic carcinoma (NACC)

No	Age	Sex	Clinical symptoms	Duration of symptoms (months)	Mucosa changes	Nerve palsy	Antibody of EBV	Pathologic types	Stage	Treatment	Recurrence
1	51	M	Nasal obstruction; epistaxis; tinnitus in the right ear	3	Protrusion in the roof and posterior wall	$V_{1,2,3}$(+)	(−)	Cribriform	T4N0M0	Radiotherapy; adjuvant chemotherapy	No
2	56	F	Headache; bilateral tinnitus; pharyngalgia	5	Protrusion in the right wall		(−)	Tubular	T3N0M0	Radiotherapy	No
3	67	M	Nasal obstruction; epistaxis	12	Nodular tumour in the roof		(−)	Tubular	T3N0M0	Radiotherapy	Yes; 1.5 years after treatment
4	40	M	Epistaxis; bilateral hearing loss	6	Lump in the roof and posterior wall		(−)	Cribriform	T2bN0M0	Surgical resection; radiotherapy	No
5	40	M	Tinnitus in the right ear; headache	1	Protrusion in the right wall with smooth surface		(−)	Cribriform	T3N0M0	Radiotherapy	No
6	38	M	Tinnitus and hearing loss in the right ear	2	Protrusion in the right wall with smooth surface		(−)	Cribriform	T4N1M0	Radiotherapy; adjuvant chemotherapy	No
7	54	M	Tinnitus in the right ear; restriction of mouth opening	24	Protrusion in the roof and posterior wall		(−)	Tubular	T4N2M0	Radiotherapy; adjuvant chemotherapy	No
8	51	F	Headache; diplopia; facial anesthesia; hearing loss	3	Protrusion in the left wall	$V_{1,2,3}$(+)	(−)	Cribriform	T4N1M0	Radiotherapy	No
9	64	M	Epistaxis; pharyngalgia	0.5	Protrusion in the roof and posterior wall with smooth surface		(−)	Tubular	T4N0M0	Radiotherapy	No
10	25	F	Headache; tinnitus in the right ear; restriction of mouth opening	18	Protrusion in the right wall with smooth surface	V_3(+)	(−)	Solid	T4N0M1	Radiotherapy; adjuvant chemotherapy	No; with lung metastasis

Table 2. MR imaging features of 10 patients with NACC

No	Imaging pattern	Location	Shape	Margin	T1WI	T2WI	Uniformity	Contrast enhancement pattern	Encroachment of adjacent structures	Skull base	Infiltration of cranial nerves and intracal.	Lymphadenopathy
1	I	Right, roof, and posterior wall of the nasopharynx	Irregular	Unclear	Iso-intensity	Slightly hyper-tensity	Homogeneous	Strong; homogeneous	Right nasal concha; right ethmoid sinus; right maxillary sinus; right parapharyngeal space; right spatia masseterica; right pterygopalatine fossa	(+)	Right $V_{2,3}$(+); right trigeminal ganglion; mass in right temple and thickening of cerebral dura mater in right temporal pole	(–)
2	I	Right, roof, and posterior wall of the nasopharynx	Irregular	Unclear	Iso-tensity	Slightly hyper-tensity	Homogeneous	Strong; homogeneous	(–)	(+)	(–)	(–)
3	I	Right, left, and roof of the nasopharynx	Irregular	Unclear	Iso-tensity	Slightly hyper-tensity	Homogeneous	Strong; homogeneous	(–)	(+)	(–)	(–)
4	I	Right wall, right part of roof, and posterior wall of the nasopharynx	Irregular	Unclear	Iso-tensity	Slightly hyper-tensity	Homogeneous	Strong; homogeneous	Right parapharyngeal space	(–)	(–)	(–)
5	I	Roof and posterior wall of the nasopharynx	Irregular	Unclear	Iso-tensity	Slightly hyper-tensity	Heterogeneous; central necrosis	Strong; heterogeneous	Right parapharyngeal	(+)	(–)	(–)
6	IIa	Left parapharyngeal space	Regular; ovoid; 21 mm × 35 mm × 40 mm	Clear	Iso-tensity	Hyper-tensity	Heterogeneous; hypointensity separations	Strong; heterogeneous; absent in separations	Left parapharyngeal space; left spatia masseterica	(–)	(–)	(–)
7	I	Right, left roof, and posterior wall of the nasopharynx	Irregular	Unclear	Iso-tensity	Slightly hyper-tensity	Homogeneous	Strong; homogeneous	Bilateral parapharyngeal spaces, soft palate, lateral wall of the oropharynx, right spatia masseterica, and bilateral pterygopalatine fossa	(+)	Left cavernous sinus; right foramen lacerum	Left level IIa, IIb
8	IIa	Left parapharyngeal space	Regular; ovoid; 34 mm × 51 mm × 54 mm	Clear	Iso-tensity	Hyper-tensity	Heterogeneous; hypointensity separations	Strong; heterogeneous; absent in separations	Left parapharyngeal space; sphenoidal sinus	(+)	Left $V_{2,3}$(+); left trigeminal ganglion; left cavernous sinus	Left regional lymph node; left level IIa
9	I	Left, roof, and posterior wall of the nasopharynx	Irregular	Unclear	Iso-tensity	Slightly hyper-tensity	Homogeneous	Strong; homogeneous	Left parapharyngeal space; left spatia masseterica; left pterygopalatine fossa; left orbita; left wall of the oropharynx	(+)		(–)
10	IIb	Right parapharyngeal space	Irregular	Unclear	Iso-tensity	slightly hyper-tensity	Heterogeneous separations	Strong; heterogeneous; absent in separations	Right parapharyngeal space; right spatia masseterica; right pterygopalatine fossa	(+)	Right $V_{2,3}$(+); right cavernous sinus; muscular dystrophy in right masticatory muscles	(–)

ACCs and 4 cribriform ACCs. The tumors classified as morphological type 2a were both cribriform ACCs, whereas the tumor classified as morphological type 2b was solid ACC.

MRI signals of NACC Six tumors had homogeneous texture with isointense signal on pre-contrast T1WI, slightly hyperintense signal on pre-contrast T2WI, and strong enhancement on contrast-enhanced T1WI. Of 4 tumors with heterogeneous texture, 3 (cases 6, 8, and 10) had separations that were hypointense signal on pre-contrast T2WI and without enhancement on contrast-enhanced T1WI, and 1 (case 5) had central necrosis. Notably, all the tubular NACCs were homogeneous tumors on MRI, and all heterogeneous tumors with separations or central necrosis were cribriform or solid NACCs.

Local invasion and cervical lymphadenopathy Tumors in all 10 patients encroached into adjacent structures in the head and neck, including the parapharyngeal space (n = 8), skull base (n = 8), spatia masseterica (n = 5), pterygopalatine fossa (n = 4), paranasal sinus (n = 2), oropharynx (n = 2), nasal concha (n = 1), soft palate (n = 1), and orbit (n = 1) (Figures 1, 3, and 4). Five patients had intracranial involvement: 4 had tumors invaded through both the foramen rotundum and foramen ovale with thickened cranial nerves, 1 had tumors invaded through an enlarged foramen lacerum. Among these 5 patients, 2 had tubular tumors, 2 had cribriform tumors, and 1 had solid tumors. Two patients, one with a tubular tumor and the other with a cribriform tumor, had regional enlarged lymph nodes with a round or ovoid shape and without central necrosis or extracapsular neoplastic spread.

Discussion

ACC is the most common histological subtype of salivary gland malignancies, but it is very rare in the nasopharynx, with relatively few cases reported in the literature. To our knowledge, the current study is one of

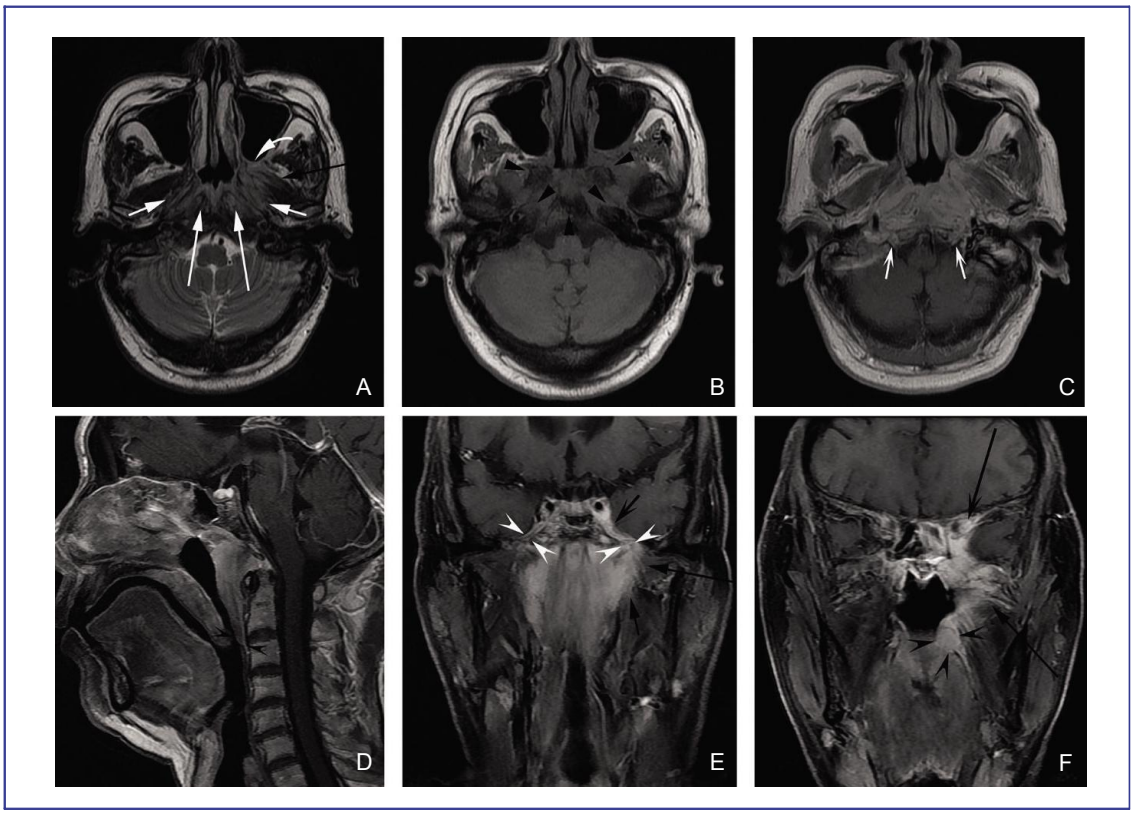

Figure 4. **MR images of a 64-year-old man with tubular NACC.** A, an axial T2W fast spin-echo image; B, an axial T1W fast spin-echo image; C, an axial contrast-enhanced T1W spin-echo image; D, a sagittal contrast-enhanced T1W spin-echo image; E, a coronal contrast-enhanced spin-echo image; F, a coronal fat-suppressed T1W image. These images show the tumor invading into bilateral parapharyngeal spaces (white arrows), bilateral retropharyngeal spaces and longus scapitis (long white arrows), left pterygopalatine fossa (curved white arrow), left medial pterygoid (black arrow), left lateral pterygoid (long black arrows), skull base bones (black arrowheads), oropharynx wall (concave black arrowheads), left cavernous sinus (concave black arrow), left orbit (long concave black arrow), bilateral mandibular nerves (concave white arrowheads), and bilateral hypoglossal canals (concave white arrows).

the largest retrospective studies summarizing the MRI features of NACC published to date. Our study indicated the following: (1) NACC was a local, aggressive neoplasm with negative laboratory test results for EBV infection and low incidence of cervical lymphadenopathy; (2) MRI features of NACC were various, depending on different locations and histiological subtypes; and (3) MRI was a valuable tool for diagnosis, tumor staging, and prognosis prediction of NACC.

Clinical characteristics of NACC

ACC predominantly occurs in adults, with a peak incidence in the fourth through sixth decades of life[10]. In accordance with the literature, the median age of patients with NACCs in this study was 51 years. Furthermore, ACC was reported to be more common in women in the literature[6,10], but there was a male predominance for NACC in the present study. Similar to NSCCs, NACCs vary in presentation from an asymptomatic mass to severe ear and neurological symptoms, such as ear pain, fullness, tinnitus, glue ear, dizziness, hearing loss, facial pain, unilateral migraine-like headache, paresthesias, numbness, sensory loss across the trigeminal nerve course, and abducens or oculomotor nerve deficits[5]. In our patients, tinnitus, headache, epistaxis, and hearing loss were the most common clinical symptoms. Trigeminal paralysis was also found in 3 patients. In accordance with the previous report by Liu *et al.*[6], none of our patients tested positive for EBV antibodies, indicating that EBV had no close relationship to the incidence of NACC. Notably, unlike the appearance of patients with NPSCC, some patients with NACC had smooth mucosal surfaces, though with protrusions in the walls of nasopharynx. We hypothesize that this is partly because NACC originates in the minor salivary glands of the submucosal region of the nasopharyngeal cavity and/or parapharyngeal space. Tumors with invasion to the nasopharyngeal mucosa may have unsmooth mucosal surfaces, whereas tumors without invasion to mucosa may have smooth mucosal surfaces.

The three main histological patterns of ACC, tubular, cribriform, and solid[11], reflect various degrees of progression of cellular differentiation and aggressiveness of biological behavior. The tubular subtype is the most differentiated form and the second most frequent, and the cribriform subtype is less differentiated than the tubular subtype and the most common pattern. The least differentiated and thus the most malignant and aggressive form is the solid subtype, accounting for 10% of ACC cases[12]. In this study, significant correlation between these histological patterns and NACC prognosis could not be demonstrated because of the small number of cases and the short time of follow-up. However, the only patient with solid NACC in our series had lung metastasis at the first visit, which might suggest the aggressive propensity of the solid subtype.

The main therapy for NACC is surgical resection[13,14]. Today, skull base surgery facilitates total resection of limited NACC lesions. The main problem is the high local recurrence rate due to invasion to the cranial nerves. Advanced tumors, especially those with skull base invasion and intracranial involvement, are difficult to resect completely. Neutron radiotherapy is also used to treat NACC. Buchholz *et al.*[15] reported that the local control rate of patients with head and neck ACC was approximately 100% for a 5-year period. In our study, 9 of 10 patients underwent radiotherapy alone or in combination with chemotherapy due to advanced tumor stage and high incidence of cranial nerve infiltration and intracranial involvement.

MRI features of NACC

Accurate pretreatment imaging diagnosis and initial imaging evaluation of NACC are necessary not only in the selection of treatment strategies, but also in the guidance of surgical resection and definition of target volume in radiotherapy. In recent years, accumulated MRI data of nasopharyngeal tumors suggest that MRI is currently the best technique for achieving an accurate diagnosis and evaluation of nasopharyngeal neoplasm extension. Previous reports of MRI on head and neck ACC showed that MRI had advantages in the detection, display of the extent, and staging of tumors[3,4]. NACC is a malignancy of the minor salivary glands, which exist in two areas of the nasopharynx: the submucosal regions of pharyngonasal cavity and the parapharyngeal space. In our patients, the tumors with a type 1 imaging pattern might originate in the former location, whereas the tumors with a type 2 imaging pattern might originate in the latter. On MR images, NACCs that originated in the submucosal minor salivary glands tended to be irregular lesions with unclear margin. On the contrary, those that originated in the minor salivary glands of the parapharyngeal space often had a regular shape and clear margin. Sigal *et al.*[3] found that signal intensity on the T2-weighted images correlated with the degree of cellularity of head and neck ACC. Tumors with high signal intensity corresponded to lesions with low cellularity, which was associated with the best prognosis. In contrast, lesions with low signal intensity correlated with dense cellularity and poor outcome. In our patients, all tubular NACCs appeared as lesions with homogeneous and slightly hyperintense signal, whereas 3 of 5 cribriform NACCs and the only solid NACC exhibited hypointense signal separations or central necrosis on T2-weighted images. Thus, these results

likely corroborate the relationship between signal intensity and cellularity.

NACC has a high potential for local invasion. Similar to patients presenting with NSCC, local NACC spreads stepwise from proximal sites to more distal sites. The parapharyngeal space, skull base, and spatia masseterica were the most common sites invaded by NACC in our study. Sigal *et al.*[3] found that MR images might cause misdiagnosis of the severity of head and neck ACCs, especially in skull base invasion. Changes in signal intensity on MR images might be caused by direct extension of the tumor to the skull base but also by edematous changes.

ACC is well known for its propensity to spread through the nerves. In the present study, 40% (4/10) of patients with NACC had cranial nerve infiltration. Notably, only 3 had clinical nerve palsy. Several studies reported that neoplasms might exist in the nerves shown up on MR images but didn't produce symptoms for many years[4,16]. There may be two reasons for this phenomenon. One is that tumors spread through the perineural space without involvement of nerve fiber. Misdiagnosis on MRI is also responsible for detection of more cranial nerve infiltration than pathologic examination. Inflammatory or edematous enlargement of the nerves may simulate neural extension of tumors on MR images. Nerve enlargement and contrast enhancement are suggestive of NACC, but perineural extension is not specific and may be seen in other neoplasms such as SCC, which is the most common neoplasm of the nasopharynx. In a previous study, Liang *et al.*[7] found that 26.4% of patients with NSCC had tumor infiltration in the mandibular branch of the trigeminal nerve.

NACC has a low incidence of cervical lymphadenopathy, accounting for only 20% (2/10) of the cases in the present study. Liu *et al.*[6] and Wang *et al.*[17] reported that the incidence of cervical metastasis in patients with NACC were 3.8% and 15%, respectively, which were much lower than other malignancies of the nasopharynx such as NSCC (64.7%–78.3%)[18,19] and nasopharyngeal non-Hodgkin's lymphoma (71.6%)[20, 21].

NACC with a type 1 imaging pattern must be radiologically differentiated from inflammatory disease, such as nasopharyngeal adenoid hyperplasia, and other malignancies, including NSCC and nasopharyngeal non-Hodgkin's lymphoma. Adenoid hyperplasia usually manifests as symmetrical thickening of the roof and posterior wall of the nasopharynx with homogeneous signal intensity on MR images and without deep invasion to adjacent tissues. In patients with NSCC, positive laboratory test results for EBV infection[22] and metastasis of regional lymph nodes are much more frequent than in patients with NACC. Diffuse and symmetrical tumors in the nasopharyngeal cavity without deep invasion, diffuse and bilateral cervical lymphadenopathy, and involvement of palatine tonsils are the characteristics of patients with nasopharyngeal non-Hodgkin's lymphoma[20,21]. In abstract, NACC with a type 2 imaging pattern must be differentiated from other tumors in the parapharyngeal space, such as neurogenic tumors and pleomorphic adenoma of the minor salivary glands. However, because of their hypointense signal separations on T2-weighted images, strong ability for local invasion, and propensity for invading cranial nerves, this type of NACC is relatively easy to differentiate from those tumor types.

The limitations of this study included: (1) that because the disease is rare, the patient cohort was too small to draw definitive conclusions from; and (2) that although the current MRI methods employed in the study provided useful information, functional MRI, such as diffusion, perfusion, and MR spectroscopy, would provide additional insight into NACC. Studies of NACC with large sample size and functional imaging methods should be carried out in the future.

Conclusions

NACC is a local, aggressive neoplasm with negative laboratory test results for EBV infection and a low incidence of cervical lymphadenopathy. MRI is a valuable tool not only for diagnosis and tumor staging, but also for prognosis prediction of NACC.

Received: 2011-06-08; revised: 2011-09-01;
accepted: 2011-10-31.

References

[1] Batsakis JG, Luna MA, El-Naggar A. Histopathologic grading of salivary gland neoplasms: III. Adenoid cystic carcinomas. Ann Otol Rhinol Laryngol, 1990,99(12):1007–1009.
[2] He J H, Zong YS, Luo R Z, et al. Clinicopathological characteristics of primary nasopharyngeal adenocarcinoma. Ai Zheng, 2003,22(7):753–757. [in Chinese]
[3] Sigal R, Monnet O, de Baere T, et al. Adenoid cystic carcinoma of the head and neck: evaluation with MR imaging and clinical-pathologic correlation in 27 patients. Radiology, 1992,184(1):95–101.
[4] Nemzek WR, Hecht S, Gandour-Edwards R, et al. Perineural spread of head and neck tumors: how accurate is MR imaging? Am J Neuroradiol, 1998,19(4):701–706.
[5] Papadas T, Chorianopoulos D, Mastronikolis N. Nasopharyngeal adenoid cystic carcinoma: a rare nasopharyngeal tumor. Eur Rev Med Pharmacol Sci, 2007,11(1):55–57.
[6] Liu TR, Yang AK, Guo X, et al. Adenoid cystic carcinoma of

the nasopharynx: 27-year experience. Laryngoscope, 2008,118 (11):1981–1988.
[7] Liang SB, Sun Y, Liu LZ, et al. Extension of local disease in nasopharyngeal carcinoma detected by magnetic resonance imaging: improvement of clinical target volume delineation. Int J Radiat Oncol Biol Phys, 2009,75(3):742–750.
[8] Gregoire V, Levendag P, Ang KK, et al. CT-based delineation of lymph node levels and related CTVs in the node-negative neck: DAHANCA, EORTC, GORTEC, NCIC, RTOG consensus guidelines. Radiother Oncol, 2003,69(3):227–236.
[9] Kimura Y, Sumi M, Sakihama N, et al. MR imaging criteria for the prediction of extranodal spread of metastatic cancer in the neck. Am J Neuroradiol, 2008,29(7):1355–1359.
[10] Rapidis AD, Givalos N, Gakiopoulou H, et al. Adenoid cystic carcinoma of the head and neck. Clinicopathological analysis of 23 patients and review of the literature. Oral Oncol, 2005,41 (3):328–335.
[11] Perzin KH, Gullane P, Clairmont AC. Adenoid cystic carcinomas arising in salivary glands: a correlation of histologic features and clinical course. Cancer, 1978,42(1):265–282.
[12] Spiro RH, Huvos AG, Strong EW. Adenoid cystic carcinoma: factors influencing survival. Am J Surg, 1979,138(4):579–583.
[13] Jr Schramm VL, Imola MJ. Management of nasopharyngeal salivary gland malignancy. Laryngoscope, 2001,111 (9):1533–1544.
[14] Qing J, Zhang Q, Wei MW, et al. Prognostic analysis of adenoid cystic carcinoma of major salivary glands of 64 cases. Ai Zheng, 2006,25(9):1138–1143. [in Chinese]
[15] Buchholz TA, Shimotakahara SG, Jr Weymuller EA, et al. Neutron radiotherapy for adenoid cystic carcinoma of the head and neck. Arch Otolaryngol Head Neck Surg, 1993,119 (7): 747–752.
[16] Liu L, Liang S, Li L, et al. Prognostic impact of magnetic resonance imaging-detected cranial nerve involvement in nasopharyngeal carcinoma. Cancer, 2009,115(9):1995–2003.
[17] Wang CC, See L , Hong J , et al. Nasopharyngeal adenoid cystic carcinoma: five new cases and a literature review. J Otolaryngol, 1996,25(6):399–403.
[18] Mao YP, Liang SB, Liu LZ, et al. The N staging system in nasopharyngeal carcinoma with radiation therapy oncology group guidelines for lymph node levels based on magnetic resonance imaging. Clin Cancer Res, 2008,14(22):7497–7503.
[19] Liu LZ, Zhang GY, Xie CM, et al. Magnetic resonance imaging of retropharyngeal lymph node metastasis in nasopharyngeal carcinoma: patterns of spread. Int J Radiat Oncol Biol Phys, 2006,66(3):721–730.
[20] King AD, Lei KI, Richards PS, et al. Non-Hodgkin's lymphoma of the nasopharynx: CT and MR imaging. Clin Radiol, 2003,58 (8):621–625.
[21] Liu XW, Xie CM, Mo YX, et al. Magnetic resonance imaging features of nasopharyngeal carcinoma and nasopharyngeal non-Hodgkin's lymphoma: are there differences? Eur J Radiol, 2011 Aug 22. [Epub ahead of print]
[22] Liu Y, Fang Z, Liu L, et al. Detection of Epstein-Barr virus DNA in serum or plasma for nasopharyngeal cancer: a meta-analysis. Genet Test Mol Biomarkers, 2011,15(7–8):495–502.